Inorganica Chimica Acta, 148 (1988) 71–84

Synthesis and Characterization of Two Isomers of $Os_3(CO)_{10}(C_5H_4N$-2-C(H)=N–R) and the Conversion to *ortho*-Metallated $HOs_3(C_5H_3N$-2-C(H)=N–R)$(CO)_9$. Part III*. X-ray Structure of $HOs_3(C_5H_3N$-2-C(H)=N–i-Pr$)(CO)_9$

ROBERT ZOET, GERARD VAN KOTEN, KEES VRIEZE**

Anorganisch Chemisch Laboratorium, University of Amsterdam, Nieuwe Achtergracht 166, 1018 WV Amsterdam, The Netherlands

ALBERT J. M. DUISENBERG and ANTHONY L. SPEK

Vakgroep Algemene Chemie, afdeling Kristal- en Structuurchemie, University of Utrecht, Padualaan 8, 3508 TB Utrecht, The Netherlands

(Received November 24, 1987)

Abstract

$Os_3(CO)_{10}(MeCN)_2$ reacts at room temperature in MeCN or toluene with R-Pyca† to yield two isomers of $Os_3(CO)_{10}$(R-Pyca) that differ in the bonding of the R-Pyca ligand to the $Os_3(CO)_{10}$ unit. In all cases $Os_3(CO)_{10}$(R-Pyca(4e)) (isomer **A**; **4a**: R = c-Pr, **4b**: R = i-Pr, **4c**: R = neo-Pent, **4d**: R = t-Bu), containing a chelating 4e donating R-Pyca ligand and three Os–Os bonds, could be isolated. In the case of R = c-Pr and R = i-Pr $Os_3(CO)_{10}$(R-Pyca(6e)) (isomer **B**; **5a**: R = c-Pr, **5b**: R = i-Pr), in which only two Os–Os bonds are present and the R-Pyca ligand is bonded as a 6e donating ligand bridging two non-bonded Os atoms, could be isolated as a minor product.

At 70 °C $Os_3(CO)_{10}$(R-Pyca(4e)) (**4b** and **4d**) loses one carbonyl and the pyridine moiety of the R-Pyca ligand is *ortho*-metallated to form $HOs_3(C_5H_3N$-2-C(H)=N–R$)(CO)_9$ (**6b**: R = i-Pr and **6d**: R = t-Bu). Under the same conditions $Os_3(CO)_{10}$(i-Pr-Pyca(6e)) (**5b**) reacts to $Os_2(CO)_6$(i-Pr-Pyca(6e)) (**7b**) containing a bridging 6e donating ligand. The latter two reactions were followed with FT-IR spectroscopy in a high temperature IR cell.

The structures of the complexes in solution have been studied by ^1H and ^{13}C NMR and IR spectroscopy. The stoichiometries of **4a** and **5a** were determined by FAB-mass spectrometry while an exact mass determination was carried out for **4a**.

The crystal structure of **6b** has been determined. Crystals of **6b** are monoclinic, space group $P2_1/n$, with $a = 7.808(2)$, $b = 17.613(3)$, $c = 16.400(8)$ Å, $\beta = 94.09(3)°$ and $Z = 4$. The structure was refined to $R = 0.039$. The molecule contains a triangular array of osmium atoms [Os(1)–Os(2) = 2.898(2) Å, Os(1)–Os(3) = 2.886(2) Å and Os(2)–Os(3) = 2.911(2) Å] and nine terminally bonded carbonyl ligands. The C_5H_3N-2-C(H)=N–i-Pr ligand is chelate bonded to Os(2) with the pyridine and imine nitrogens atoms axially and equatorially coordinated respectively [Os(2)–N(1) = 2.00(2) Å and Os(2)–N(2) = 2.11(2) Å]. The i-Pr-Pyca ligand is *ortho*-metallated at C(1) and forms a four membered ring containing Os(2), Os(3), C(1) and N(1), the Os(3)–C(1) distance being 2.12(2) Å. The hydride, which could not be located unequivocally from a difference Fourier map, is proposed to bridge the Os(2)–Os(3) bond on the basis of stereochemical considerations.

Introduction

A previous study of the reactions of R-DAB† with $Os_3(CO)_{10}(MeCN)_2$ has demonstrated the flexible coordination behaviour of the R-DAB ligand with respect to trinuclear osmium carbonyl compounds. Two isomers of $Os_3(CO)_{10}$(R-DAB), *i.e.* $Os_3(CO)_{10}$(R-DAB(4e)) (compound **1**, isomer **A**) and $Os_3(CO)_{10}$(R-DAB(6e)) (compound **2**, isomer **B**) were isolated (see Scheme 1) [1].

The first isomer, $Os_3(CO)_{10}$(R-DAB(4e)) (compound **1**, isomer **A**), contains a chelating 4e donating R-DAB ligand and a closed metal triangle with three metal–metal bonds. In the second isomer, $Os_3(CO)_{10}$-

*Part III: for earlier parts see refs. 1 and 2.

**Author to whom correspondence should be addressed.

†Pyridine-2-carbaldimines 6-R^1–C_5H_3N-2-C(H)=N–R are abbreviated as R-Pyca{R^1}. When R^1 = H the abbreviation R-Pyca can be used. 1,4-disubstituted-1,4-diaza-1,3-butadienes; R–N=C(H)–C(H)=N–R are abbreviated as R-DAB. The number of electrons donated by the ligands to the cluster is indicated between brackets, *i.e.* α-diimine(4e) stands for σ,σ-N,N chelating 4e coordinated, which coordination mode is also denoted as isomer **A**; α-diimine(6e) stands for σ-N,μ_2-N′,η^2-C=N′ bridging 6e coordinated, which coordination mode is denoted as isomer **B**; α-diimine(8e) stands for σ,σ-N,N′-η^2,η^2-C=N,C′=N′ 8e bridging coordinated.

0020-1693/88/$3.50

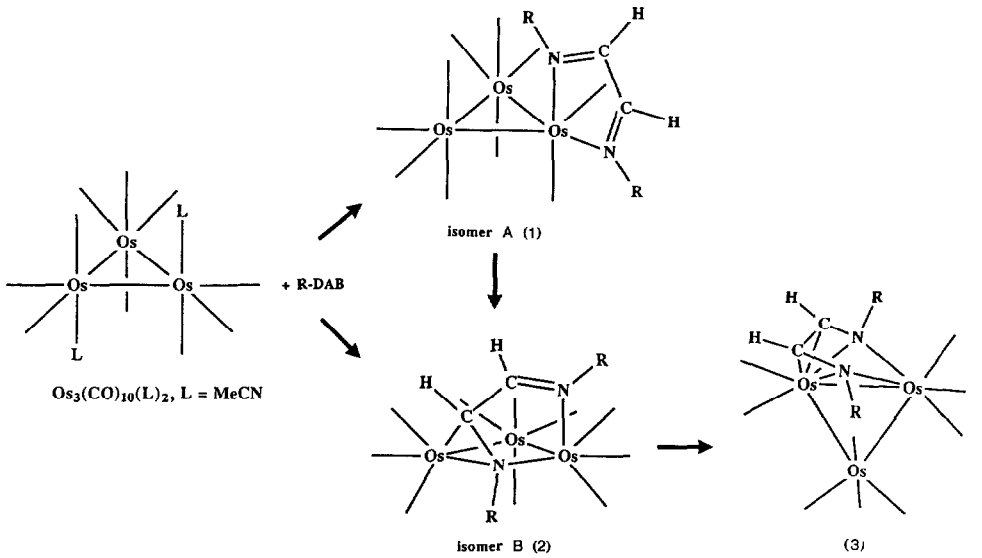

Scheme 1. The $Os_3(CO)_{10}(MeCN)_2$/R-DAB reaction sequence. $Os_3(CO)_{10}$(R-DAB(4e)) (1b and 1c), $Os_3(CO)_{10}$(R-DAB(6e)) (2a and 2b) and $Os_3(CO)_9$(R-DAB(8e)) (3a and 3b) (a: R = c-Pr, b: R = i-Pr, c: R = neo-Pent and d: R = t-Bu).

(R-DAB(6e)) (compound 2, isomer **B**), also one of the π-imine bonds is coordinated which results in a bridging 6e donating R-DAB ligand and a total electron count of fifty for the trinuclear cluster. The Os–Os bond bridged by the R-DAB ligand is broken which is in accordance with CVMO theory that predicts only two metal–metal bonds for a trinuclear 50e compound. Interestingly for R = neo-Pent only $Os_3(CO)_{10}$(neo-Pent-DAB(4e) (isomer **A**) and for R = c-Pr only $Os_3(CO)_{10}$(c-Pr-DAB(6e)) (isomer **B**) was obtained. For R = i-Pr an intriguing solvent effect on the product distribution was observed. When the reaction was performed in coordinating solvents such as THF and MeCN, $Os_3(CO)_{10}$(i-Pr-DAB(4e)) (isomer **A**) was the main product whereas in toluene $Os_3(CO)_{10}$(i-Pr-DAB(6e)) (isomer **B**) was formed predominantly.

On thermolysis in refluxing hexane $Os_3(CO)_{10}$(i-Pr-DAB(4e)) (isomer **A**) reacted via $Os_3(CO)_{10}$(i-Pr-DAB(6e)) (isomer **B**) and subsequent elimination of one carbonyl ligand to $Os_3(CO)_9$(i-Pr-DAB(8e)) (**3b**) (see Scheme 1) [2]. A crystal structure determination of **3b** showed that in this compound the lone pairs of both nitrogens and the π-electrons of both imine bonds of the R-DAB ligand are donated to the cluster core and hence the ligand donates a total of 8e to the cluster. The cluster has a valence shell electron count of 50 electrons and instead of rupturing one Os–Os bond, as would be expected, two Os–Os bonds are elongated analogous to the Ru–Ru bond lengthening found in $Ru_3(CO)_9$(R-DAB(8e)) [3]. Apparently, the LUMO is easily accessible which renders the 50e situation with an 8e donating R-DAB ligand more stable than the 48e situation with a 6e donating R-DAB ligand.

These results prompted us to investigate the reactions of R-Pyca with $Os_3(CO)_{10}(MeCN)_2$. The R-Pyca ligand is of particular interest since it can act as a 2e, 4e or 6e donor [4, 5, 6a–c] but very likely not as an 8e donor, since π-coordination of one C=N moiety of the pyridine ring would cause loss of resonance stabilization energy. A further point of interest is that by the incorporation of the C=N moiety in the pyridine ring and the possibility to introduce substituents on the pyridine ring the type of coordination can be affected by means of electronic and steric factors.

In this article we present the formation of $Os_3(CO)_{10}$(R-Pyca) which, in analogy to $Os_3(CO)_{10}$(R-DAB), may occur in two isomeric forms, *i.e.* isomer **A** and **B** of Scheme 2. Furthermore the conversion of $Os_3(CO)_{10}$(R-Pyca(4e)) and $Os_3(CO)_{10}$(R-Pyca(6e)) by means of thermolysis reactions to $HOs_3(C_5H_3N\text{-}2\text{-}C(H)=N\text{–}R)(CO)_9$ and $Os_2(CO)_6$(R-Pyca(6e)) respectively, are reported. These thermolysis reactions will be compared with the strikingly different thermolysis behaviour of $Os_3(CO)_{10}$(R-DAB(4e)) and of $Os_3(CO)_{10}$(R-DAB(6e)) which has been reported previously.

Experimental

Materials and Apparatus

^1H and ^{13}C NMR spectra were obtained on a Bruker AC100 and WM250 spectrometer. IR spectra were recorded with a Perkin-Elmer 283 spectrophotometer. FT-IR spectra were obtained on a Nicolet 7199b FT-IR interferometer (liquid nitrogen cooled Hg, Cd, Te detector; 32 scans, resolution = 0.5

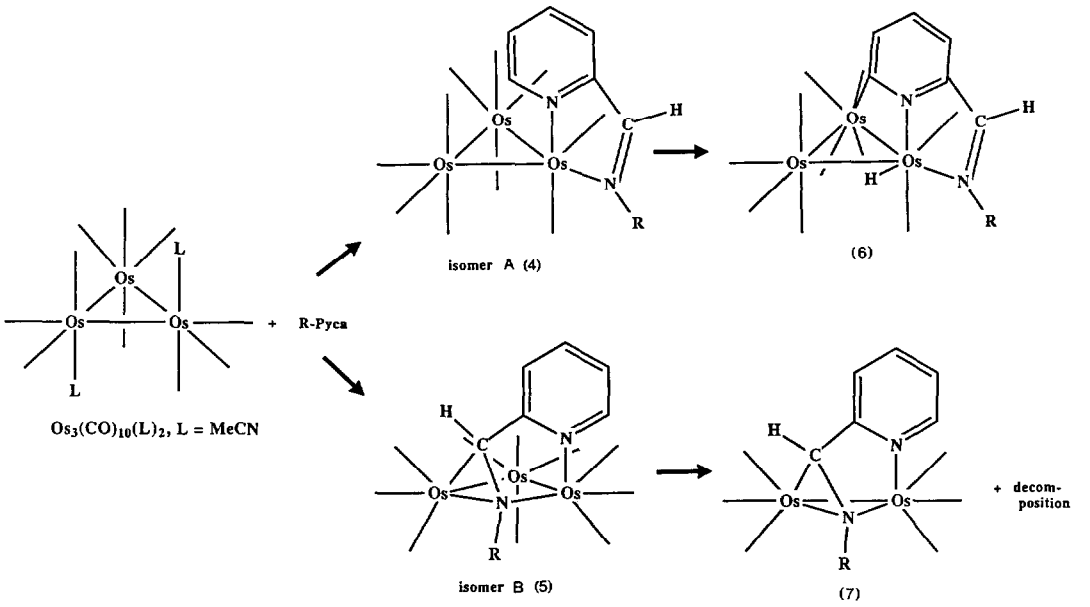

Scheme 2. The $Os_3(CO)_{10}(MeCN)_2$/R-Pyca reaction sequence. $Os_3(CO)_{10}$(R-Pyca(4e)) (**4a**, **4b**, **4c** and **4d**), $Os_3(CO)_{10}$(R-Pyca(6e)) (**5a** and **5b**), $HOs_3(C_5H_3N\text{-}2C(H)=N-R)(CO)_9$ (**6b** and **6d**) and $Os_2(CO)_6$(R-Pyca(6e)) (**7b**) (a: R = c-Pr, b: R = i-Pr, c: R = neo-Pent and d: R = t-Bu).

cm^{-1}). For the high temperature experiments a Beckman variable temperature unit VLT-2 was used with a FH-01 VT-cell and CsI windows (0.1 mm pathlength). Field desorption (FD) mass spectra were obtained with a Varian MAT 711 double focussing mass spectrometer with a combined EI/FD/FI ion source and coupled to spectro system MAT 100 data acquisition unit [7]. Fast Atom Bombardment (FAB) mass spectrometry was carried out using a VG micromass ZAB-2F mass spectrometer, an instrument with reverse geometry and fitted with a high field magnet and coupled to a VG 11-250 data system. The samples were loaded in thioglycerol onto a stainless steel probe and bombarded with xenon atoms having 8 KeV energy. During the high resolution FAB-MS measurements a resolving power of 25 000 (10% valley definition) was used. Elemental analyses were carried out by the section Elemental Analyses of the Institute of Applied Chemistry, TNO, Zeist, The Netherlands. All preparations were carried out in an atmosphere of purified nitrogen, using carefully dried solvents. Silica gel (60 Mesh) for column chromatography was activated before use. Chromatography columns of 30 cm length and a diameter of 2 cm were used. The R-Pyca ligands (a: R = c-Pr; b: R = i-Pr; c: R = neo-Pent; d: R = t-Bu) were prepared according to literature methods [8a–c] and for the synthesis of $Os_3(CO)_{10}(MeCN)_2$ a modified literature procedure was used [1].

Synthesis of $Os_3(CO)_{10}$(R-Pyca)

R-Pyca (a: R = c-Pr, b: R = i-Pr, c: R = neo-Pent, d: R = t-Bu; 0.12 mmol) was added to a stirred suspension of $Os_3(CO)_{10}(MeCN)_2$ (0.11 mmol) in MeCN at room temperature or in toluene at −20 °C. When the reaction was performed in toluene the suspension was allowed in 2 h to warm to room temperature. The colour of the reaction mixture turned blue. It was stirred for 4 h at room temperature. The solvent was evaporated and the residue was dissolved in 0.5 ml of CH_2Cl_2 and separated by column chromatography. In the case of c-Pr and i-Pr a yellow product was obtained in minor yield by elution with hexane: diethyl ether = 4:1. It was identified as $Os_3(CO)_{10}$(c-Pr-Pyca(6e)) (**5a**) and $Os_3(CO)_{10}$(i-Pr-Pyca(6e)) (**5b**). In all cases with hexane:diethyl ether = 1:2 as eluent the $Os_3(CO)_{10}$(R-Pyca(4e)) (**4a**, **4b**, **4c** and **4d**) complexes were obtained. The eluent was evaporated to 10 ml and the product precipitated as crystals upon cooling to −80 °C. The solvent was decanted and the crystals were dried *in vacuo*. Yield of $Os_3(CO)_{10}$(c-Pr-Pyca(4e)) (**4a**) 0.002 mmol (18%); $Os_3(CO)_{10}$(i-Pr-Pyca(4e)) (**4b**) 0.05 mmol (45%); $Os_3(CO)_{10}$(neo-Pent-Pyca(4e)) (**4c**) 0.05 mmol (45%); $Os_3(CO)_{10}$(t-Bu-Pyca(4e)) (**4d**) 0.04 mmol (36%); $Os_3(CO)_{10}$(c-Pr-Pyca(6e)) (**5a**) and $Os_3(CO)_{10}$(i-Pr-Pyca(6e)) (**5b**) 0.002 mmol (2%).

Synthesis of $HOs_3(C_5H_3N\text{-}2\text{-}C(H)=N-R)(CO)_9$ (6b: R = i-Pr, 6d: R = t-Bu)

Compound **4b** or **4d** (0.05 mmol) was refluxed for 24 h in n-hexane until IR spectroscopy indicated that the ν(CO) pattern of the starting material had been replaced by that of **6b** or **6d**. The colour of the solution remained blue. The isolation and purification procedure was the same as above with the exception

that on chromatography these complexes were eluted with hexane:diethyl ether = 1:1. Yield of both **6b** and **6d** 0.015 mmol (30%).

FT-IR Spectroscopy of the Conversion of 4b to 6b and 5b to 7b

For the FT-IR measurements at 80 °C the FH-01 VT variable temperature infrared cell was filled with a solution of either **4b** or **5b** in n-nonane. This high boiling solvent was chosen to avoid as much as possible the evaporation of the solvent during the measurements since the cell was not sealed for the reason that carbon monoxide must be able to evolve from the solution. The cell was placed in the corresponding vessel, which was flushed with nitrogen, and was heated in 15 min to the reaction temperature after which spectra were recorded every 15 min. The temperature of the cell was kept constant within a range of 1.5 °C. In following the conversion of **4b** a smooth disappearance of the starting material was observed together with the formation of **6b** and some $Os_3(CO)_{12}$ (see Fig. 1). In the case of **5b** extensive decomposition as well as the formation of **7b** was observed (see Fig. 2). Although no precise kinetic details could be obtained, owing to slow evaporation of solvent, the available data indicate that the reactions are first order in complex.

Crystal Structure Determination of $HOs_3(C_5H_3N\text{-}2\text{-}C(H)\text{=}N\text{-}i\text{-}Pr)(CO)_9$ (6b), $Os_3C_{18}H_{12}N_2O_9$

Crystal data and numerical details of the structure determination are listed in Table I. X-ray data were collected on an Enraf-Nonius CAD4F diffractometer for a dark-red–brown crystal mounted on top of a glass fibre. Reflection profiles were highly structured. Unit cell parameters were derived by least-squares from the diffractometer settings of 25 reflections [9a] in the range $18° < 2\theta < 32°$ and checked with rotation photographs about the three axes. The space group was derived from the observed systematic extinctions. Three reference reflections showed no decay over the 89 h of X-ray exposure time. Data were corrected for Lp and for absorption with a Gaussian integration procedure (8 X 8 X 8 grid; min. and max. correction 3.87 and 15.10 resp.) and averaged ($R_{av}(I) = 6.79\%$). The structure was solved by Patterson methods with the program SHELXS84 [9b] and refined on F by full-matrix least-squares on a MicroVAX II with SHELX76 [9c]. sp^2 C–H phenyl H atoms and sp^3 H atoms were introduced at calculated positions [d(C–H) = 1.08 Å] and refined with fixed geometry with respect to their carrier atoms. The hydride could not be identified unequivocally in a difference map but was introduced with slack constraints in a bridging position over Os(2)–Os(3).

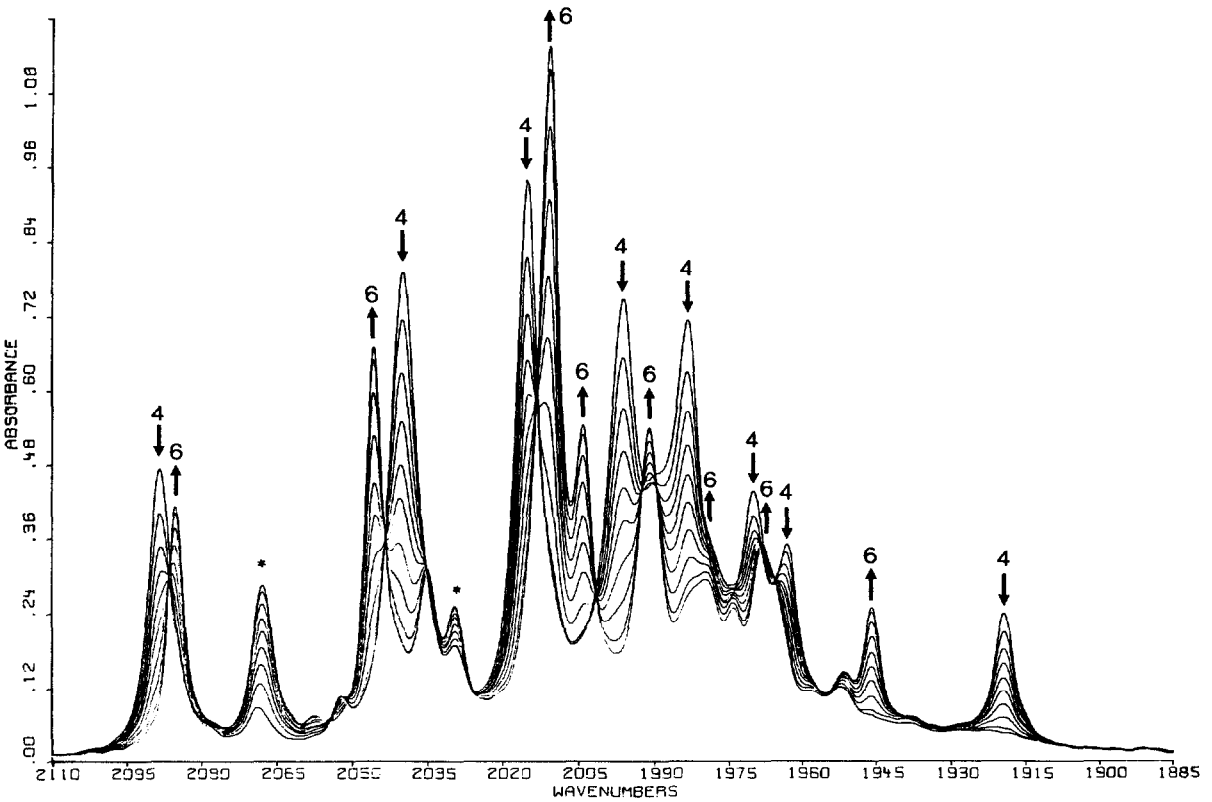

Fig. 1. Conversion of $Os_3(CO)_{10}$(i-Pr-Pyca)(4e)) (**4b**) to $Os_3(CO)_{10}$(i-Pr-Pyca)(6e)) (**6b**) followed with FT-IR spectroscopy as a function of time. Bands marked with an asterisk are assigned to $Os_3(CO)_{12}$.

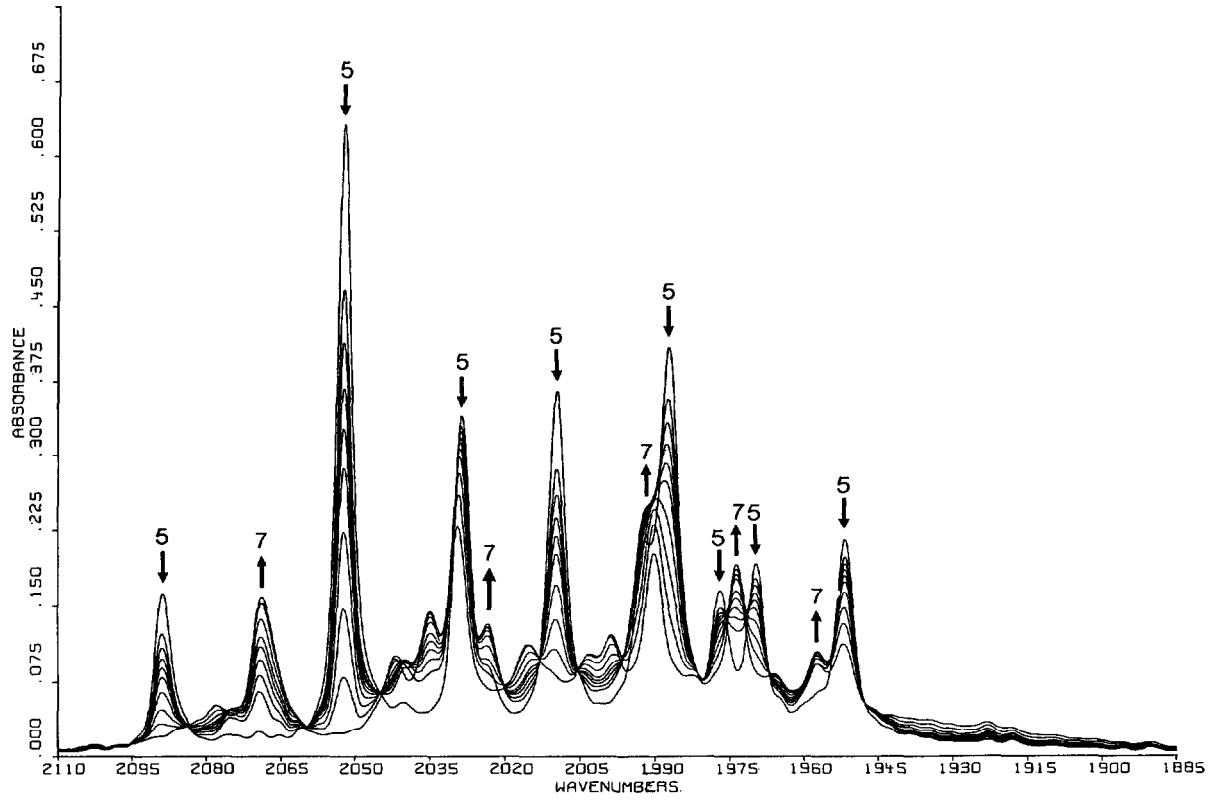

Fig. 2. Conversion of $Os_3(CO)_{10}$(i-Pr-Pyca(6e)) (**5b**) to $Os_2(CO)_6$(i-Pr-Pyca(6e)) (**7b**) followed with FT-IR spectroscopy as a function of time.

The Os–H distance refined to 1.83 Å with U = 0.02(4) Å^2. The refined parameter set included a scale factor, the coordinates of the non-hydrogen atoms, their anisotropic thermal parameters and three separate isotropic temperature factors for the H atoms.

Final positional parameters for the non-hydrogen atoms are listed in Table II. Scattering factors were taken from the literature [9d,e] and corrected for anomalous dispersion [9f]. The calculation of geometrical data and the preparation of illustrations were carried out with the programs PLATON and PLUTON of the EUCLID-package [9g]. The molecular geometry of **6b** with the numbering of the atoms is given in Fig. 3, which shows a PLUTON drawing of the molecule. Bond lengths and bond angles are given in Tables III and IV respectively.

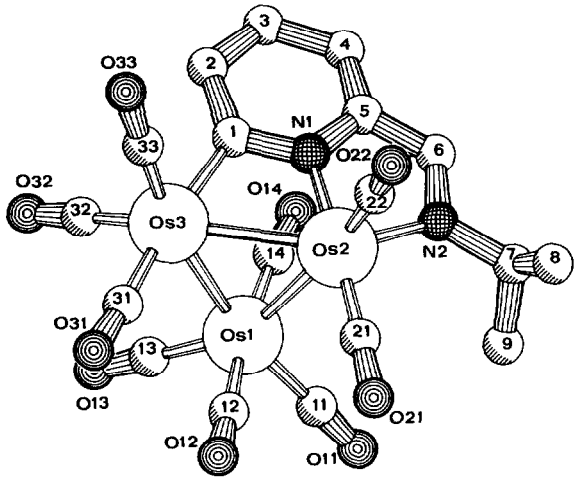

Fig. 3. The molecular geometry of $HOs_3(C_5H_3N$-2-C(H)=N–i-Pr)$(CO)_9$ (**6b**).

Results and Discussion

Formation of Products

The formation of the $Os_3(CO)_{10}$(R-Pyca) complexes (**a**: R = c-Pr; **b**: R = i-Pr; **c**: R = neo-Pent; **d**: R = t-Bu) together with their schematic structures are depicted in Scheme 2.

The reactions of $Os_3(CO)_{10}(MeCN)_2$ with R-Pyca were carried out in MeCN or toluene at room temperature. However, the reactions in toluene were vigorous and extensive decomposition was observed when they were started at room temperature. Better yields were obtained when the reactions in toluene

TABLE I. Crystal Data and Details of the Structure Determination of $HOs_3(C_5H_3N\text{-}2\text{-}C(H)=N\text{-}i\text{-}Pr)(CO)_9$ (6b)

Crystal data	
Formula	$C_{18}H_{12}N_2O_9Os_3$
Molecular weight	970.91
Space group	$P2_1/n$
a (Å)	7.808(2)
b (Å)	17.613(3)
c (Å)	16.400(8)
β (°)	94.09(3)
V (Å^3)	2250(1)
Z	4
D_x (g cm^{-3})	2.866
F(000), electrons	1736
μ(Mo Kα) (cm^{-1})	169.7
Crystal size (mm)	1 1 0 (–) –1 –1 0 0.125 –1 1 0 (–) 1 –1 0 0.125 0 0 1 (–) 0 0 –1 0.425
Data collection	
Temperature (°)	295
Radiation	Zr-filtered Mo Kα, λ = 0.71073 Å
θ_{min}, θ_{max} (°)	1.16, 22.0
ω scan (°)	$\Delta\omega = 2.00 + 0.35 \tan\theta$
Horizontal and vertical apertures (mm)	3, 3
Data set	$-8 \leq h \leq 8$, $-18 \leq k \leq 18$, $0 \leq l \leq 17$
Reference reflections	1 1 0; 0 2 1; 1 0 –3
Total data, unique data	5765, 2749
Observed data ($I > 2.5\sigma(I)$)	2088
Refinement	
No. refined parameters	302
Weighting scheme	$w^{-1} = \sigma^2(F) + 0.001F^2$
R, R_w	0.039, 0.054
Min., max. resid. density (e/Å^3)	–1.30, 1.48

TABLE II. Positional and Equivalent Isotropic Thermal Parameters of $HOs_3(C_5H_3N\text{-}2\text{-}C(H)=N\text{-}i\text{-}Pr)(CO)_9$ (6b)

Atom	x	y	z	U_{eq} [a] (Å^2)
Os(1)	0.0626(1)	0.12938(5)	0.33968(5)	0.0382(3)
Os(2)	–0.1238(1)	0.16798(5)	0.18616(5)	0.0325(3)
Os(3)	–0.1803(1)	–0.02260(5)	0.26424(5)	0.0339(3)
O(11)	0.278(4)	0.271(1)	0.390(1)	0.12(1)
O(12)	–0.239(3)	0.197(1)	0.427(1)	0.09(1)
O(13)	0.185(2)	0.021(1)	0.476(1)	0.074(6)
O(14)	0.343(2)	0.083(1)	0.231(1)	0.10(1)
O(21)	–0.291(3)	0.292(1)	0.275(1)	0.083(8)
O(22)	–0.405(2)	0.183(1)	0.052(1)	0.082(8)
O(31)	–0.436(2)	0.050(1)	0.3927(9)	0.060(6)
O(32)	–0.012(2)	–0.1080(9)	0.362(1)	0.057(6)
O(33)	–0.429(3)	–0.069(1)	0.152(1)	0.071(8)
N(1)	0.007(2)	0.084(1)	0.1368(9)	0.040(6)
N(2)	0.065(2)	0.2225(9)	0.1209(9)	0.035(6)
C(1)	–0.017(2)	0.015(1)	0.167(1)	0.034(6)
C(2)	0.068(3)	–0.050(1)	0.132(1)	0.044(8)
C(3)	0.189(3)	–0.037(1)	0.074(1)	0.05(1)
C(4)	0.217(3)	0.040(1)	0.049(1)	0.05(1)
C(5)	0.122(3)	0.097(1)	0.083(1)	0.040(8)
C(6)	0.154(3)	0.177(1)	0.074(1)	0.041(6)
C(7)	0.102(4)	0.305(1)	0.115(1)	0.053(8)
C(8)	–0.044(4)	0.346(1)	0.074(2)	0.08(1)
C(9)	0.150(4)	0.339(1)	0.195(1)	0.07(1)
C(11)	0.200(4)	0.219(2)	0.371(1)	0.07(1)
C(12)	–0.135(4)	0.174(1)	0.394(2)	0.06(1)
C(13)	0.141(3)	0.061(2)	0.426(2)	0.06(1)
C(14)	0.231(3)	0.098(1)	0.270(1)	0.05(1)
C(21)	–0.224(3)	0.244(1)	0.239(1)	0.05(1)
C(22)	–0.290(3)	0.178(1)	0.099(1)	0.040(6)
C(31)	–0.334(4)	0.041(1)	0.346(1)	0.050(8)
C(32)	–0.072(3)	–0.059(1)	0.325(1)	0.05(1)
C(33)	–0.341(3)	–0.031(1)	0.196(1)	0.05(1)

[a] $U_{eq} = 1/3\Sigma_i\Sigma_j U_{ij} a_i^* a_j^* \vec{a}_i \vec{a}_j$.

TABLE III. Bond Distances (Å) of the Atoms of $HOs_3(C_5H_3N\text{-}2\text{-}C(H)=N\text{-}i\text{-}Pr)(CO)_9$ (6b)[a]

Os(1)–Os(2)	2.898(2)	Os(3)–C(31)	1.89(2)	N(1)–C(1)	1.33(2)
Os(1)–Os(3)	2.886(2)	Os(3)–C(32)	1.91(2)	N(1)–C(5)	1.32(3)
Os(1)–C(11)	1.96(3)	Os(3)–C(33)	1.88(2)	N(2)–C(6)	1.34(2)
Os(1)–C(12)	2.00(3)	O(11)–C(11)	1.13(4)	N(2)–C(7)	1.49(2)
Os(1)–C(13)	1.93(3)	O(12)–C(12)	1.09(4)	C(1)–C(2)	1.46(3)
Os(1)–C(14)	1.89(2)	O(13)–C(13)	1.12(4)	C(2)–C(3)	1.41(3)
Os(2)–Os(3)	2.911(2)	O(14)–C(14)	1.15(3)	C(3)–C(4)	1.44(3)
Os(2)–N(1)	2.00(2)	O(21)–C(21)	1.18(3)	C(4)–C(5)	1.39(3)
Os(2)–N(2)	2.11(2)	O(22)–C(22)	1.14(3)	C(5)–C(6)	1.44(3)
Os(2)–C(21)	1.80(2)	O(31)–C(31)	1.15(3)	C(7)–C(8)	1.47(4)
Os(2)–C(22)	1.87(2)	O(32)–C(32)	1.14(2)	C(7)–C(9)	1.47(2)
Os(3)–C(1)	2.12(2)	O(33)–C(33)	1.17(3)		

[a] e.s.d.s given in parentheses.

TABLE IV. Bond Angles (°) of the Atoms of $HOs_3(C_5H_3N\text{-}2\text{-}C(H)=N\text{-}i\text{-}Pr)(CO)_9$ (**6b**)[a]

Os(2)–Os(1)–Os(3)	60.43(4)	Os(2)–Os(3)–C(32)	144.6(7)
Os(2)–Os(1)–C(11)	105.7(7)	Os(2)–Os(3)–C(33)	107.2(5)
Os(2)–Os(1)–C(12)	86.5(9)	C(1)–Os(3)–C(31)	173.1(7)
Os(2)–Os(1)–C(13)	154(1)	C(1)–Os(3)–C(32)	94.4(8)
Os(2)–Os(1)–C(14)	82.6(6)	C(1)–Os(3)–C(33)	86.1(8)
Os(3)–Os(1)–C(11)	165.8(8)	C(31)–Os(3)–C(32)	92.2(8)
Os(3)–Os(1)–C(12)	86.7(8)	C(31)–Os(3)–C(33)	94(1)
Os(3)–Os(1)–C(13)	94.1(9)	C(32)–Os(3)–C(33)	100.7(8)
Os(3)–Os(1)–C(14)	90.8(6)	Os(2)–N(1)–C(1)	116(1)
C(11)–Os(1)–C(12)	90(1)	Os(2)–N(1)–C(5)	122(1)
C(11)–Os(1)–C(13)	100(1)	C(1)–N(1)–C(5)	122(2)
C(11)–Os(1)–C(14)	90(1)	Os(2)–N(2)–C(6)	115(1)
C(12)–Os(1)–C(13)	98(1)	Os(2)–N(2)–C(7)	129(1)
C(12)–Os(1)–C(14)	169(1)	C(6)–N(2)–C(7)	116(2)
C(13)–Os(1)–C(14)	94(1)	Os(3)–C(1)–N(1)	109(1)
Os(1)–Os(2)–Os(3)	59.59(4)	Os(3)–C(1)–C(2)	131(1)
Os(1)–Os(2)–N(1)	86.5(4)	N(1)–C(1)–C(2)	119(2)
Os(1)–Os(2)–N(2)	102.8(4)	C(1)–C(2)–C(3)	119(2)
Os(1)–Os(2)–C(21)	88.0(6)	C(2)–C(3)–C(4)	118(2)
Os(1)–Os(2)–C(22)	164.8(6)	C(3)–C(4)–C(5)	118(2)
Os(3)–Os(2)–N(1)	68.0(5)	N(1)–C(5)–C(4)	123(2)
Os(3)–Os(2)–N(2)	139.1(4)	N(1)–C(5)–C(6)	112(2)
Os(3)–Os(2)–C(21)	110.9(6)	C(4)–C(5)–C(6)	124(2)
Os(3)–Os(2)–C(22)	107.5(6)	N(2)–C(6)–C(5)	115(2)
N(1)–Os(2)–N(2)	74.7(6)	N(2)–C(7)–C(8)	111(2)
N(1)–Os(2)–C(21)	174.0(8)	N(2)–C(7)–C(9)	112(1)
N(1)–Os(2)–C(22)	96.1(7)	C(8)–C(7)–C(9)	110(2)
N(2)–Os(2)–C(21)	104.4(8)	Os(1)–C(11)–O(11)	179(2)
N(2)–Os(2)–C(22)	92.4(7)	Os(1)–C(12)–O(12)	177(3)
C(21)–Os(2)–C(22)	89.8(8)	Os(1)–C(13)–O(13)	179(2)
Os(1)–Os(3)–Os(2)	59.98(4)	Os(1)–C(14)–O(14)	174(2)
Os(1)–Os(3)–C(1)	87.2(5)	Os(2)–C(21)–O(21)	178(2)
Os(1)–Os(3)–C(31)	90.9(7)	Os(2)–C(22)–O(22)	172(2)
Os(1)–Os(3)–C(32)	90.8(6)	Os(3)–C(31)–O(31)	176(2)
Os(1)–Os(3)–C(33)	167.2(5)	Os(3)–C(32)–O(32)	178(2)
Os(2)–Os(3)–C(1)	66.8(5)	Os(3)–C(33)–O(33)	174(2)
Os(2)–Os(3)–C(31)	106.6(5)		

[a]e.s.d.s given in parentheses.

were commenced at −20 °C followed by stirring at room temperature.

$Os_3(CO)_{10}$(R-Pyca(4e)) (**4**) complexes, containing a chelating 4e donating R-Pyca ligand, were isolated for all R substituents, while for R = c-Pr and i-Pr also $Os_3(CO)_{10}$(R-Pyca(6e)) (**5**) complexes were isolated in minor amounts. It is concluded on the basis of available spectroscopic data (*vide infra*) that complexes **4** and **5** are isostructural with $Os_3(CO)_{10}$(R-DAB(4e)) (**1**) and $Os_3(CO)_{10}$(R-DAB(6e)) (**2**), respectively (Scheme 1).

Upon refluxing in n-hexane **4b** and **4d** converted to $HOs_3(C_5H_3N\text{-}2\text{-}C(H)=N\text{–}R)(CO)_9$ (**6b**: R = i-Pr and **6d**: R = t-Bu respectively; Scheme 2). In this reaction one CO molecule is lost and the pyridine moiety of the R-Pyca ligand is *ortho*-metallated with the two nitrogen atoms still σ,σ-N,N′ coordinated to the same osmium atom. A careful examination of the thermolysis reaction of $Os_3(CO)_{10}$(i-Pr-Pyca(4e)) (**4b**) by means of following the reaction in a high temperature IR cell indicated that **4b** converted directly to $HOs_3(C_5H_3N\text{-}2\text{-}C(H)=N\text{–}R)(CO)_9$ (**6b**), while the formation of the intermediate $Os_3(CO)_{10}$(i-Pr-Pyca(6e)) (**5b**) was not observed.

Because of the small quantity of **5b** that was available for studying its behaviour on thermolysis (since it was obtained in only 2% yield), its further reaction could only be investigated by following the reaction in a variable temperature IR cell. It was observed that on thermolysis **5b** gave cluster breakdown to dinuclear $Os_2(CO)_6$(i-Pr-Pyca(6e)) (**7b**), with a 6e donating i-Pr-Pyca ligand, together with unidentified decomposition products (see Scheme 2). Complex **7b** is isostructural with $Os_2(CO)_6$(R-DAB(6e)) which was synthesized by the reaction of $Os_3(CO)_{12}$ and R-DAB [10]. In the course of the reaction the $Os(CO)_4$ unit

of **5b** is eliminated and an Os–Os bond is formed between the two osmium atoms that are bridged by the i-Pr-Pyca ligand.

Before considering the reaction routes in more detail the identification of the products by ^{1}H NMR, ^{13}C NMR, IR, and mass spectroscopy and the molecular structure of the *ortho*-metallated **6b** will be discussed.

Molecular Geometry of $HOs_3(C_5H_3N$-2-C(H)=N–i-Pr)$(CO)_9$ (6b)

The molecular geometry of **6b** together with the atomic numbering is given in Fig. 3. The bond lengths and angles are given in Tables III and IV.

As shown in Fig. 3 **6b** consists of a triangular array of osmium atoms. Os(1) is linked to four terminal carbonyl ligands, Os(2) is linked to two carbonyl ligands and the two nitrogen atoms of the monoanionic tridentate C_5H_3N-2-C(H)=N–i-Pr ligand while Os(3) is linked to three carbonyl ligands and C(1) of the metallated pyridine ring. Consequently, a five membered chelate ring at Os(2) is present which is fused with the four membered metallocyclic ring comprising Os(2), Os(3), C(1) and N(1). The imine nitrogen atom of the C_5H_3N-2-C(H)=N–i-Pr ligand resides in the equatorial position, while the pyridine nitrogen atom is axially bonded to Os(2). The latter bond is significantly shorter [Os(2)–N(2) = 2.11(2) Å *versus* Os(2)–N(1) = 2.00(2) Å]. The axial CO ligand bonded to Os(2), *trans* to N(1), experiences a greater π-backdonation from osmium and is associated with a shorter Os–C bond [Os(2)–C(21) = 1.80(2) Å]. The Os(3)–C(1) distance of 2.12(2) Å in **6b** is similar to the distance of 2.118(12) Å found for $HOs_3(C_{10}H_7N_2)(CO)_9$ [11]. The latter compound is of particular interest since it contains a *ortho*-metallated bipyridine ligand that is bonded like the C_5H_3N-2-C(H)=N–i-Pr ligand in **6b**.

The hydride could not be located unequivocally but bridges most probably Os(2) and Os(3) as can be inferred from stereochemical evidence. These structural features were deduced from a large number of molecular structure determinations of clusters of the type $HOs_3(CO)_{10}X$ (where X is a monoatom or double atom bridging ligand; for example Cl or C=N respectively) that have been undertaken by Churchill *et al.* [12a–c]. In the first place the hydride is normally found to bridge the same Os–Os bond as X. When X is a double atom bridge, as in the present case, the bridged Os–Os distance is the longest. The observed Os–Os distances in **6b** are in accordance with this. The two non-bridged Os–Os distances are of normal length for an Os–Os single bond [Os(1)–Os(2) = 2.898(2) Å and Os(1)–Os(3) = 2.886(2) Å] while the Os pair bridged by the CN donor sites and the hydride is longer [Os(2)–Os(3) = 2.911(2) Å], as compared to 2.8771(27) Å for $Os_3(CO)_{12}$ [12a]. Other examples are $HOs_3(C_{10}H_7N_2)(CO)_9$ and $HOs_3(MeN{=}COC(O)N(H)Me)(CO)_{10}$ [13]. For the latter compound the bridging hydride was located. Secondly it is observed that the carbonyls neighbouring a bridging hydride are pushed aside. In **6b** the Os(2)–Os(3)–C(31) and Os(3)–Os(2)–C(21) angles of the axial CO ligands have increased to 106.6(5)° and 110.9(6)° respectively. Similarly increased angles were found in, for example, $H_2Os_3(CO)_{11}$ [12a] and $HOs_3(MeN{=}COC(O)N(H)Me)(CO)_{10}$.

Within the ligand the imine bond length C(6)–N(2) of 1.34(2) Å is rather long as compared to the imine bond length of 1.258(3) Å in the free c-Hex-DAB ligand [4] but similar to the imine bond length of 1.31(3) Å in the chelate coordinated R-DAB ligand in $Os_3(CO)_{10}$(i-Pr-DAB(4e)) [1]. The structural features of the bridging CN moiety of **6b** are related to several other complexes containing a Os(μ-H)(μ-C=N)Os bridge as, for example, $HOs_3(MeN{=}COC(O)N(H)Me)(CO)_{10}$, $HOs_3((CF_3)C{=}NH)(CO)_9(P(Me)_2Ph)$ [14a], $HOs_3(PhC{=}NMe)(CO)_{10}$ [14b], $HOs_3(HC{=}NPh)(CO)_9(P(OMe)_3)$ [14c] and $HOs_3(C_{10}H_7N_2)(CO)_9$.

Mass Spectroscopy

The results of the FD mass measurements are summarized in Table V. The trinuclear character of the complexes is clearly indicated by the observed isotope patterns. The molecular ion is observed to have the highest intensity and the observed masses are, within experimental error, in accord with the calculated molecular weights.

Of the complexes **4a** and **5a** also FAB mass spectra were recorded together with an exact mass measurement for **4a**. For **4a** the isotopic pattern of the molecular ion was found around *m/z* 998 and the loss of eight carbonyls was observable. The exact mass of 1001.9543 (based on ^{192}Os) measured for **4a** was within experimental error of the calculated mass (1001.9180, based on ^{192}Os for $Os_3C_{19}H_{10}N_2O_{10}$). Also for complex **5a** the isotopic pattern of the molecular ion was found around *m/z* 998. In this case the loss of nine carbonyls was observable. However, due to fragmentation the intensity of the peak of the molecular ion was too weak for an exact mass determination. Apparently **5a**, containing only two Os–Os bonds, is in the gas phase less stable than **4a** that has three Os–Os bonds.

IR, ^{1}H NMR and ^{13}C NMR Spectroscopy

The absorptions in the ν(CO) region in the IR spectrum are listed in Table V. The ^{1}H and ^{13}C NMR data of the complexes are listed in Tables VI and VII, respectively. Schematic structures of the complexes **1** to **7** are depicted in Schemes 1 and 2.

$Os_3(CO)_{10}$(R-Pyca(4e)) (4a, 4b, 4c and 4d)

The resonances for the imine hydrogens and carbons in the ^{1}H and ^{13}C NMR spectra of **4a** to **4d**

TABLE V. IR and FD Mass Spectral Data

Compound	R group	FD-MS[a]	ν(CO)[b]
4a	c-Pr	1000 (998)	2086, 2038, 2014, 1997, 1984, 1978, 1960, 1922
4b	i-Pr	1001 (1000)	2086, 2038, 2014, 1996, 1982, 1969, 1962, 1919
4c	t-Bu	1015 (1014)	2084, 2037, 2011, 1997, 1983, 1971, 1960, 1917
4d	neo-Pent	1001 (1028)[d]	2085, 2036, 2012, 1997, 1983, 1971, 1962, 1918
5a	c-Pr	999 (998)	2085, 2050, 2023, 2004, 1986, 1975, 1967, 1945[c]
5b	i-Pr	999 (1000)	2086, 2049, 2026, 2008, 1987, 1977, 1969, 1951
6a	i-Pr	972 (972)	2083, 2043, 2009, 2005, 1991, 1982, 1968, 1945
6d	t-Bu	987 (986)	2080, 2041, 2006, 2004, 1989, 1980, 1966, 1942
7b	i-Pr		2065, 2024, 1988, 1972, 1950

[a]Observed (calculated). The measured and calculated values account for the highest peak in the measured and simulated isotope pattern. [b]In hexane (cm^{-1}). [c]In CH_2Cl_2. [d]Peak due to $[M - CO]^+$.

are found at 8 and 157 ppm, respectively. These chemical shifts are indicative for the σ,σ-N,N' coordination mode of the R-Pyca ligand [15]. The σ,σ-N,N' coordination is further supported by the IR spectra of **4a** to **4d** which show an absorption pattern in the ν(CO) region similar to that of $Os_3(CO)_{10}$(i-Pr-DAB(4e)) (**1b**) [1]. The crystal structure determination of **1b** particularly showed that the imine nitrogens of the bidentate bonded i-Pr-DAB ligand are spanning one equatorial and one axial coordination site. Consequently it seems reasonable to assume that in **4a** to **4d** the pyridine and imine nitrogens are likewise axially and equatorially coordinated. It is proposed on the basis of the presence of the sterically bulky R group on the imine nitrogen atom, that it is the imine site that is in an equatorial position while the pyridine nitrogen atom is coordinated to the axial position. It is generally observed that sterically more bulky groups prefer equatorial positions [16]. It may be expected that **4** is involved in a similar fluxional process as was observed for **1b**. Unfortunately it appeared that the solubility of **4** was too low for performing variable temperature NMR experiments.

$Os_3(CO)_{10}$(R-Pyca(6e)) (5a and 5b)

For **5a** and **5b** the resonances of the imine hydrogens were found around 3.9 ppm. Such an upfield shift is indicative for a η^2-C(H)=N coordination of the imine bond and is a common feature for all compounds containing 6e donor α-diimine ligands which have been studied so far. [5, 10, 17a–c]. Thus the observed resonance indicates that in **5a** and **5b** the ligand is in a bridging 6e coordination mode. A second indication for this is the similarity of the IR spectra of **5a**, **5b** and the analogous R-DAB compounds **2a** and **2b**. A molecular structure determination for **2a** has been performed showing that it contains a bridging 6e donating c-Pr-DAB ligand and two Os–Os bonds. We may therefore conclude that **5a**, **5b**, **2a** and **2b** have analogous structures as depicted in Schemes 1 and 2.

Metallated Os compounds (6b and 6d)

In the ^{1}H NMR of $HOs_3(CO)_9(C_5H_3N$-2-C(H)=N–R) (**6b** and **6d**) the doublet of the proton at the 6-position of the pyridine ring has disappeared leaving two doublets and one triplet for the protons at the 5, 3 and 4 positions respectively. The resonance of the hydride is found as a singlet at −20.19 and −20.83 ppm for **6b** and **6d** respectively, which is indicative for a hydride in a bridging position [18]. The imine protons of **6b** and **6d** absorb at 6.51 and 6.92 ppm respectively, as expected for a σ-N coordination of the carbaldehydeimine part of the R-Pyca ligand [15].

$Os_2(CO)_6$(t-Bu-Pyca(6e)) (7b)

The structure of **7b** can be deduced from its IR spectrum, which shows a ν(CO) pattern similar to that observed for other $M_2(CO)_6$(α-diimine) (M = Fe, Ru, Os) complexes containing a bridging, 6e donating α-diimine ligand [5, 10].

Reaction Pathways in the System $Os_3(CO)_{10}(MeCN)_2$/(α-diimine)

Of central interest in the reaction system $Os_3(CO)_{10}(MeCN)_2$/R-Pyca are (i) the routes and intermediates via which the two isomers $Os_3(CO)_{10}$(R-Pyca(4e)) (isomer **A**) and $Os_3(CO)_{10}$(R-Pyca(6e)) (isomer **B**) are formed and (ii) the *ortho*-metallation reaction which converts $Os_3(CO)_{10}$(R-Pyca(4e)) into $HOs_3(C_5H_3N$-2C(H)=NR)$(CO)_9$ (**3**).

(i) Reaction of $Os_3(CO)_{10}(MeCN)_2$ with R-Pyca

To discuss the reaction of $Os_3(CO)_{10}(MeCN)_2$ with R-Pyca it is essential to compare this system with the results obtained for the reactions of $Os_3(CO)_{10}(MeCN)_2$ with R-DAB, which show interesting analogies but also differences.

In Scheme 3 important features of the R-DAB system are displayed and it is useful to discuss first some essential points regarding this reaction system. As in the case of R-Pyca two isomers are formed that

TABLE VI. ^{1}H NMR Data[a]

Compound		Pyridine H peaks				R group	Imine-H	Hydride
		H(6)	H(3)	H(4)	H(5)			
4a[b]	c-Pr	9.40(d, 7 Hz, 1 H)	8.01(d, 8 Hz, 1 H)	7.82(dd, 8 Hz, 1 H)	7.17(dd, 7 Hz, 1 H)	1.27(m, 4 H) 4.06(m, 1 H)	8.79(s, 1 H)	
4b[c]	i-Pr	9.29(d, 6 Hz, 1 H)	6.77(d, 7 Hz, 1 H)	6.62(dd, 7 Hz, 1 H)	6.01(dd, 6 Hz, 1 H)	0.92(d, 7 Hz, 3 H)/ 1.06(d, 7 Hz, 3 H); 4.46(sept, 7 Hz, 1 H)	7.94(s, 1 H)	
4c[b]	neo-Pent	9.43(d, 6 Hz, 1 H)	8.02(d, 7 Hz, 1 H)	7.81(dd, 7 Hz, 1 H)	7.17(dd, 6 Hz, 1 H)	1.09(s, 9 H) 3.97(d, 12 Hz, 1 H)/ 4.36(d, 12 Hz, 1 H)	8.57(s, 1 H)	
4d[b]	t-Bu	9.42(d, 6 Hz, 1 H)	8.07(d, 7 Hz, 1 H)	7.90(dd, 7 Hz, 1 H)	7.18(dd, 6 Hz, 1 H)	1.63(s, 9 H)	8.97(s, 1 H)	
5a[c, d]	c-Pr	7.78(d, 6 Hz, 1 H)	6.43(d, 7 Hz, 1 H)	6.52(dd, 7 Hz, 1 H)	5.91(dd, 6 Hz, 1 H)	0.89(m, 4 H) 2.45(m, 1 H)	3.87(s, 1 H)	
5b[c]	i-Pr	7.78(d, 6 Hz, 1 H)	6.53(d, 7 Hz, 1 H)	6.57(dd, 7 Hz, 1 H)	5.98(dd, 6 Hz, 1 H)	0.60(d, 6 Hz, 3 H)/ 1.10(d, 6 Hz, 3 H); 1.49(sept, 6 Hz, 1 H)	3.99(s, 1 H)	
6b[c, d]	i-Pr	–	6.67(d, 8 Hz, 1 H)	6.49(vt, 8 Hz, 1 H)	6.22(d, 8 Hz, 1 H)	1.03(d, 6 Hz, 3 H)/ 1.08(d, 6 Hz, 3 H) 3.41(sept, 7 Hz, 1 H)	6.51(s, 1 H)	−20.19(s, 1 H)
6d[c, d]	t-Bu	–	6.79(d, 8 Hz, 1 H)	6.56(vt, 8 Hz, 1 H)	6.27(d, 8 Hz, 1 H)	1.13(s, 1 H)	6.92(s, 1 H)	−20.83(s, 1 H)

[a]Chemical shift in ppm downfield from TMS, s = singlet, d = doublet, dd = doublet of doublet, sept = septet, m = multiplet, vt = virtual triplet, J in Hz. Recorded at 100 MHz. [b]Solvent CD_2Cl_2. [c]Solvent C_6D_6. [d]Recorded at 250 MHz.

TABLE VII. ^{13}C NMR Data[a]

Compound		Pyridine					R group	Imine
		C2	C6	C3	C4	C5		
4a	c-Pr	155.6	155.6	135.4	128.1	124.2	50.1; 13.0; 11.2	156.2
4b	i-Pr	156.3	155.1	135.6	128.1	124.3	67.8; 26.9; 21.4	156.2
4c	neo-Pent	155.2	156.0	135.1	127.4	123.9	78.8; 34.2; 28.1	159.9
4d	t-bu	157.2	156.3	136.5	128.8	124.6	68.7; 32.7	159.3
6b	i-Pr	160.5	158.0	138.1	135.3	124.0	70.4; 27.4; 26.3	159.3
6d	t-Bu	160.4	159.7	138.3	135.3	124.5	69.6; 33.8	159.7

[a]Chemical shift in ppm downfield from TMS, solvent CD_2Cl_2.

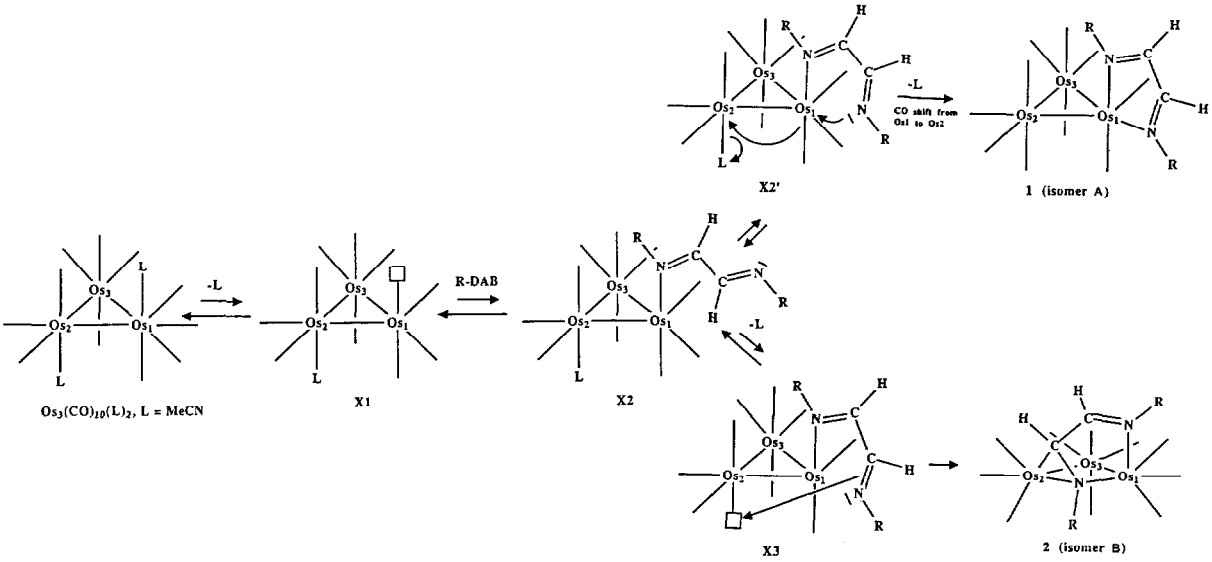

Scheme 3. Proposed mechanism for the formation of $Os_3(CO)_{10}$(R-DAB(4e)) (1) and $Os_3(CO)_{10}$(R-DAB(6e)) (2).

differ with respect to the number of electrons donated to the $Os_3(CO)_{10}$ unit, *i.e.* 4 electrons (isomer **A**) and 6 electrons (isomer **B**). The product ratio of these isomers depends predominantly on the substituent R and to a lesser extent on the solvent and on the reaction temperature. Use of small R groups (e.g. i-Pr or c-Pr) led predominantly to the formation of the isomer **B** with a 6e donor R-DAB and two Os–Os single bonds, while for larger R groups (i.e. neo-Pent) the formation of the isomer **A**, with a 4e donor chelating R-DAB and three Os–Os bonds was observed. This is understandable, since it is known that larger R groups tend to protect the π-C=N bond of α-diimines against coordination to a metal atom. It should be noted that t-Bu-DAB does not give any reaction at all. In the case of R = i-Pr the influence of the coordinating capacity of the solvent on the type of isomer formed became noticeable, since isomer **A** was formed in MeCN and isomer **B** in toluene.

When we now consider Scheme 3 in more detail it is reasonable to assume, as proposed by Poë *et al.*, that $Os_3(CO)_{10}(MeCN)_2$ dissociates into $Os_3(CO)_{10}$(MeCN) (**X1**), with an empty coordination position e.g. on Os(1), and MeCN [19]. Undoubtedly R-DAB will get attached in the first instance via a σ-N monodentate bonding of one of the N=C moieties as shown in intermediate **X2**. It should be noted here that the reaction in MeCN only proceeds when excess R-DAB is used since in MeCN as a solvent intermediate **X1** will be present in only a very small concentration. This also gives a rationalization for the observation that t-Bu-DAB does not react, since it is known that monodentate coordination of t-Bu-DAB is difficult to achieve owing to the large size of the t-Bu substituent [6a]. On further reaction the intermediate **X2** loses the second coordinated MeCN ligand affording intermediate **X3** with again an empty coordination position now on Os(2)*. The relative concentrations of **X2** and **X3** will depend largely on

*It has been noted by Poë *et al.* that the dissociation of this second MeCN molecule may be facilitated by the first incoming ligand. Furthermore, the carbonyl ligands will be mobile, as observed for **2b**, so the vacant coordination site can migrate over the trinuclear cluster.

the nature of the solvent. In non-coordinating solvents like toluene one may expect a relatively large amount of **X3**.

On the basis of these considerations the product formation of isomers **A** and **B** can now be explained. Comparison of **X2** and **X3** shows that when the π-C=N bond of the non-coordinated end is relatively unprotected, *i.e.* in the case of small R groups, the 6e donating R-DAB isomer **B** will be formed predominantly via a movement of the free C=N–R moiety to the empty coordination position on Os(2) with concomitant rupture of the Os(1)–Os(2) bond. Alternatively isomer **B** may also be formed from **X2** by substitution of MeCN on Os(2) by the π-C=N–R bond, but this will be a higher energy process.

For the formation of the 4e donating R-DAB isomer **A** large R groups are needed which prevent the π-C=N bond from coordination. Isomer **A** may be formed from **X2'**, by a concerted process involving a CO shift from Os(1) to Os(2) with concomitant dissociation of MeCN on Os(2) and formation of a chelating R-DAB group. Naturally isomer **A** may also be formed via intermediate **X3**, since this would only involve a CO shift from Os(1) to Os(2) and chelation of R-DAB on Os(1). Therefore it can only be concluded that isomers **A** and **B** may be formed via both intermediates **X2** and **X3**, when only the steric bulk of the R group is taken into account as a steering factor.

The situation, however, becomes more subtle, when also the influence of the nature of the solvent on the product ratio of isomers **A** and **B** for R = i-Pr is included in the discussion. The predominant formation of isomer **A** in MeCN (and THF) and the predominant formation of isomer **B** in toluene may be rationalized by assuming a difference in relative concentrations of **X2** and **X3** as a result of the different coordinating abilities of these solvents. It is likely that **X3** will be present in only a low concentration in MeCN relative to **X2**, whereas in toluene **X3** may occur in higher concentrations.

On purpose the R-DAB system has been discussed in some detail, before discussing the $Os_3(CO)_{10}$-$(MeCN)_2$/R-Pyca system, see Scheme 4.

It is of interest to note that contrary to the unreactivity of t-Bu-DAB, t-Bu-Pyca does react with $Os_3(CO)_{10}(MeCN)_2$. Furthermore, no excess of R-Pyca is needed in MeCN to obtain a reaction, in contrast to R-DAB (*vide infra*). As in the R-DAB system, isomer **A** appears to be formed not only for big R groups (t-Bu, neo-Pent), but still is the most abundant isomer when R = c-Pr or i-Pr. For the last two substituents isomer **B** could also be isolated, but only in minor amounts. Finally, there appears to be no observable influence of the solvent on the product distribution.

We may rationalize these findings as follows. The first stages of the reaction up to intermediate **X2**, will be the same. It seems reasonable to assume that, in particular when R is large, the R-Pyca ligand will become coordinated to Os(1) via the pyridine-N atom, since we do observe reactions with t-Bu-Pyca. Intermediate **X3** may be formed from **X2** by dissociation of MeCN from Os(2). As stressed before isomers **A** and **B** may be formed in principle from both intermediates **X2** and **X3**, but it is interesting that for the reactions with the R-Pyca ligands we do not see a great influence of the size of the R group on the product distribution. This may be rationalized by the steric interaction of the pyridine ring with the car-

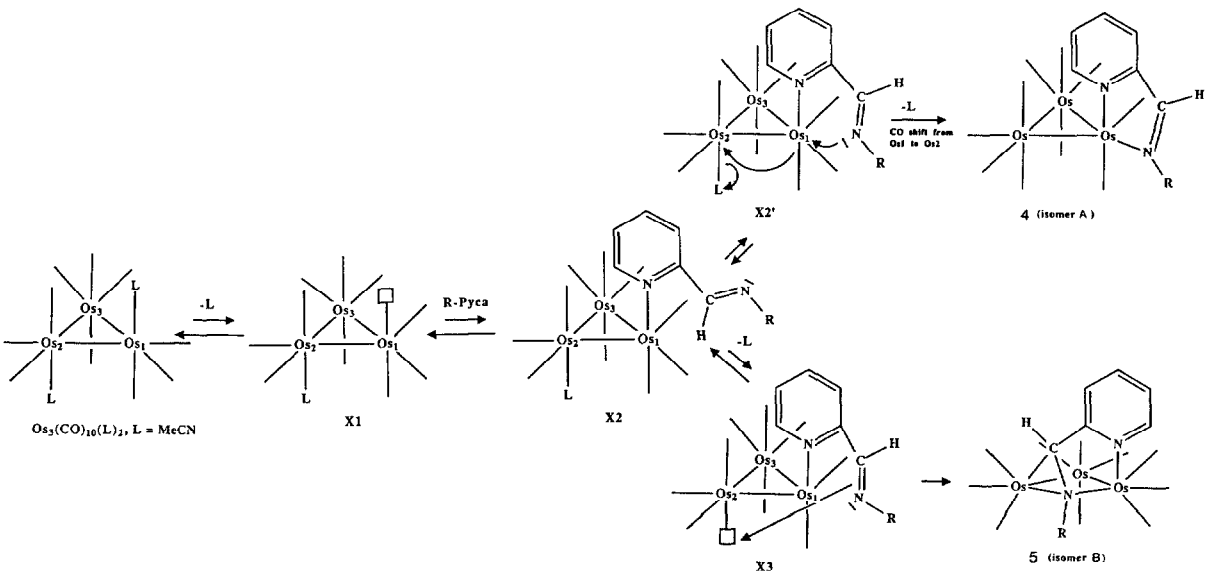

Scheme 4. Proposed mechanism for the formation of $Os_3(CO)_{10}$(R-Pyca(4e)) (4) and $Os_3(CO)_{10}$(R-Pyca(6e)) (5).

bonyl groups located on Os(2) and Os(3). Models show that such steric interactions will hinder rotation around the Os(1)–N(pyridine) bond thereby hindering attack of the π-C=N bond on Os(2). This would also explain the absence of solvent dependence, which is, however, difficult to observe in any case since the yield of isomer **B** is low.

In particular for small R groups it may be expected that intermediates of type **X2** and **X3** with a σ-monodentate bonding of the R–N=C part of the R-Pyca ligand to Os(1) could be formed. Subsequent reaction to give isomer **A** could then be explained easily by proceeding from **X2** and **X3**, but not the formation of isomer **B** for R = c-Pr and i-Pr.

Finally we may conclude that in the R-Pyca system it is most likely that the proposed intermediates (**X2**, **X3**) involve pyridine-N coordination, although σ-R–N=C coordination cannot be rigorously excluded.

(ii) ortho-Metallation of $Os_3(CO)_{10}$(R-Pyca(4e)) to $HOs_3(C_5H_3N$-2-C(H)=N–R)$(CO)_9$ (3)

In the case of $Os_3(CO)_{10}$(R-DAB) a careful investigation by means of FT-IR has shown for R = i-Pr that $Os_3(CO)_{10}$(i-Pr-DAB(4e)) (**1b**) converts at 80 °C to $Os_3(CO)_{10}$(i-Pr-DAB(6e)) (**2b**) and subsequently at 70 °C to $Os_3(CO)_9$(i-Pr-DAB(8e)) (**3b**) [1,2]. A crystal structure determination of $Os_3(CO)_9$(i-Pr-DAB(8e)) has demonstrated that the compound contains an 8e-donating i-Pr-DAB ligand with two elongated Os–Os bonds and one Os–Os bond with a normal single bond length.

Since R-Pyca has never been observed as yet to coordinate as an 8e-donor ligand, it was of interest to investigate the thermolysis of $Os_3(CO)_{10}$(R-Pyca). A FT-IR study of the thermolysis at 80 °C of $Os_3(CO)_{10}$(R-Pyca) showed that when the reaction is carried out for the 4e bonded R-Pyca isomers **A** (R = i-Pr or t-Bu), that these isomers are converted directly via an *ortho*-metallation reaction to a new compound of the composition $HOs_3(C_5H_3N$-2-C(H)=N–R)$(CO)_9$ (**6b**) and (**6d**). Although no precise quantitative data could be obtained owing to slow evaporation of the solvent, it seems reasonable to assume that the reaction has first order kinetics. For *ortho*-metallation to occur the pyridine ring should be close with its *ortho*-H atom to Os(2) or Os(3). As discussed before, such steric interaction occurs, as shown by models*. For $Os_3(CO)_{10}$(bipy) [11] and $Ru_3(CO)_{10}$(bipy) [20a, b] similar *ortho*-metallation reactions were observed**.

An attempt has been made to study the thermolysis of $Os_3(CO)_{10}$(i-Pr-Pyca(6e)) (**5b**), since the i-Pr-DAB analogue (**2b**) is an intermediate in the conversion of isomer **A** to $Os_3(CO)_9$(i-Pr-DAB(8e)) at 70 °C.

The thermolysis of **5b** could only be performed on a small scale, because of the small quantity of **5b** available. For this reason the thermolysis of a solution of **5b** was performed in a high temperature IR cell, while the reaction was followed with FT-IR spectroscopy. Of interest is that **5b** is converted, with loss of $Os(CO)_4$, to $Os_2(CO)_6$(i-Pr-Pyca(6e)) and decomposition products and not to the *ortho*-metallated compound (**6b**). From the proposed mechanism it is clear why **5b** is not converted to **6b**, since in **5b** the pyridine ring has a fixed orientation with respect to the $Os_3(CO)_{10}$ unit and is clearly not in the right position for *ortho*-metallation to occur.

Supplementary Material

Listing of elemental analysis data and listing of the hydrogen atom positions, anisotropic thermal parameters, bond distances and angles and a list of observed and calculated structure factors of **6b** are available upon request from Dr A. L. Spek.

Acknowledgements

We thank J. M. Ernsting for his assistance with the recording of the NMR spectra, G. Schoemaker for the FT-IR measurements, G.U.A. Sai for recording the FD mass spectra and R. Fokkens for the exact mass measurements. We thank Dr D. J. Stufkens for stimulating discussions. We thank the Netherlands Foundation for Chemical Research (S.O.N.) and the Netherlands Organization for Pure Research (Z.W.O.) for their financial support.

References

1 R. Zoet, D. Heijdenrijk, J. T. B. H. Jastrzebski, G. van Koten, T. Mahabiersing, C. H. Stam and K. Vrieze, *Organometallics*, accepted for publication.
2 R. Zoet, G. van Koten, C. H. Stam and K. Vrieze, *Organometallics*, accepted for publication.

*Another way of rationalizing the *ortho*-metallation reaction is to view the $Os_2(CO)_8$ fragment isolobal with ethylene that is η^2-coordinated to the $Os(CO)_2$(R-Pyca) fragment. By rotation of the $Os_2(CO)_8$ fragment the osmium atoms will come within close distance of the *ortho*-hydrogen atom of the pyridine ring which will facilitate the *ortho*-metallation reaction.

Deeming *et al.* investigated the thermolysis reaction of $Os_3(CO)_{12}$ with 2,2'-bipy at 185 °C that gave $HOs_3(CO)_9(C_{10}H_7N_2)$. The latter compound is isostructural with **6b. It seems reasonable to assume that this reaction proceeds via $Os_3(CO)_{10}$(bipy) which, under the conditions employed, reacts further to $HOs_3(CO)_9(C_{10}H_7N_2)$. A similar behaviour is observed with $Ru_3(CO)_{10}$(bipy) which reacted to $HRu_3(CO)_9(C_{10}H_7N_2)$ in refluxing toluene.

3 J. Keijsper, L. H. Polm, G. van Koten, C. H. Stam, P. F. A. B. Seignette and K. Vrieze, *Inorg. Chem., 24,* 518 (1985).
4 K. Vrieze, G. van Koten, J. Keijsper and C. H. Stam, *Polyhedron, 2,* 1111 (1983).
5 L. H. Polm, G. van Koten, C. J. Elsevier, K. Vrieze, B. F. K. van Santen and C. H. Stam, *J. Organomet. Chem., 304,* 353 (1986).
6 (a) G. van Koten and K. Vrieze, *Adv. Organomet. Chem., 21,* 151 (1982); (b) K. Vrieze, *J. Organomet. Chem., 300,* 307 (1986); (c) K. Vrieze and G. van Koten, *Inorg. Chim. Acta, 100,* 79 (1985).
7 L. H. Staal, G. van Koten, R. H. Fokkens and N. M. M. Nibbering, *Inorg. Chim. Acta, 50,* 205 (1981).
8 G. Z. Bähr and H. Thämlitz, *Z. Anorg. Allg. Chem., 282,* 3 (1955); (b) *292,* 119 (1957); (c) M. A. Robinson, J. D. Curry and D. H. Bush, *Inorg. Chem., 2,* 1178 (1963).
9 (a) J. L. de Boer and A. J. M. Duisenberg, *Acta Crystallogr., Sect. A, 40,* C410 (1984); (b) G. M. Sheldrick, 'SHELXS84', program for crystal structure determination, University of Göttingen, F.R.G.; (c) G. M. Sheldrick, 'SHELX76', crystal structure analysis package, University of Cambridge, U.K., 1976; (d) D. T. Cromer and J. B. Mann, *Acta Crystallogr., Sect. A, 24,* 321 (1968); (e) R. F. Stewart, E. R. Davidson and W. T. Simpson, *J. Chem. Phys., 42,* 3175 (1965); (f) D. T. Cromer and D. Liberman, *J. Chem. Phys., 53,* 1891 (1970); (g) A. L. Spek, The EUCLID-Package, in D. Sayre (ed.), 'Computational Crystallography', Clarendon Press, Oxford, 1982, p. 528.
10 L. H. Staal, G. van Koten and K. Vrieze, *J. Organomet. Chem., 206,* 99 (1981).
11 A. J. Deeming, R. Peters, M. B. Hursthouse and J. D. J. Backer-Dirks, *J. Chem. Soc., Dalton Trans.,* 787 (1982).
12 (a) M. R. Churchill and B. G. DeBoer, *Inorg. Chem., 16,* 878 (1977); (b) M. R. Churchill and H. J. Wasserman, *Inorg. Chem., 20,* 1580 (1981); (c) M. R. Churchill, B. G. DeBoer and F. J. Rotella, *Inorg. Chem., 15,* 1843 (1976).
13 Y. C. Lin, C. B. Knobler and H. D. Kaesz, *J. Am. Chem. Soc., 103,* 1216 (1981).
14 (a) R. D. Adams, D. A. Katahira and Li-Wu Yang, *J. Organomet. Chem., 219,* 85 (1981); (b) R. D. Adams and N. M. Golembski, *Inorg. Chem., 17,* 1969 (1978); (c) R. D. Adams and N. M. Golembski, *J. Am. Chem. Soc., 101,* 2579 (1979).
15 L. H. Staal, J. Keijsper, L. H. Polm and K. Vrieze, *J. Organomet. Chem., 204,* 101 (1981).
16 M. R. Churchill and B. G. DeBoer, *Inorg. Chem., 16,* 2397 (1977).
17 (a) L. H. Staal, J. Keijsper, G. van Koten, K. Vrieze, J. A. Cras and W. P. Bosman, *Inorg. Chem., 20,* 555 (1981); (b) L. H. Staal, L. H. Polm, R. W. Balk, G. van Koten, K. Vrieze and A. M. F. Brouwers, *Inorg. Chem., 19,* 3343 (1980); (c) L. H. Staal, L. H. Polm, K. Vrieze, F. Ploeger and C. H. Stam, *Inorg. Chem., 20,* 3590 (1981).
18 A. P. Humphries and H. D. Kaesz, *Prog. Inorg. Chem., 25,* 145 (1979).
19 K. Dahlinger, A. J. Poë, P. K. Sayal and V. C. Sekhar, *J. Chem. Soc., Dalton Trans.,* 2145 (1986).
20 (a) G. A. Foulds, B. F. G. Johnson and J. Lewis, *J. Organomet. Chem., 294,* 123 (1985); (b) G. A. Foulds, B. F. G. Johnson and J. Lewis, *J. Organomet. Chem., 296,* 147 (1985).